

Time-resolved spectra of polar-polarizable chromophores in solution

Francesca Terenziani* and Anna Painelli†

Dip. di Chimica GIAF Università di Parma, 43100 Parma, INSTM UdR Parma, Italy

A recently proposed model for steady-state spectra of polar-polarizable chromophores is extended to describe time-resolved spectra. The model, based on a two-state picture for the solute and on a continuum overdamped description for the (polar) solvent, grasps the essential physics of solvation dynamics, as demonstrated by the comparison with experimental spectra. The solute (hyper)polarizability is responsible for spectroscopic features that cannot be rationalized within the standard picture based on a linear perturbative treatment of the solute-solvent interaction. In particular, the temporal evolution of band-shapes and the appearance of temporary isosbestic points, two common puzzling features of observed spectra, are natural consequences of the molecular hyperpolarizability and of the consequent coupling between solvation and vibrational degrees of freedom.

I. INTRODUCTION

Time-resolved spectroscopy is a powerful tool to investigate solvent dynamics^{1,2}, one of the central issues in modern chemical physics, and a key to understand the rate of chemical reactions in solution^{3,4}. Detailed information on solvent dynamics can in fact be obtained from time-resolved spectra of properly chosen *probe molecules* in solution. Good solvation probes have strongly solvatochromic and intense absorption (and/or emission) bands in the visible region⁵, as not to interfere with transitions in the ultraviolet region. Polyconjugated chromophores with good electron-donor (D) and acceptor (A) groups (also called push-pull chromophores) work fine in this respect: intense and low-lying transitions are guaranteed by polyconjugation, and the large charge displacement from D to A (or viceversa) driven by the transition is responsible for a large variation of the dipole moment upon excitation, that makes the frequency of the transition largely dependent on the polarity of the surrounding medium.

In the simplest model for solvation, the solvent is described as a dielectric continuum medium hosting solute molecules into Onsager-type cavities⁶. The electric dipole moment of the (polar) solute polarizes the solvent so that the solute itself experiences an electric field, the reaction field, proportional to the solute dipole moment via a proportionality constant that depends on the macroscopic properties of the solvent, and on the shape and size of the Onsager cavity. Two contributions to the reaction field can be distinguished^{7,8}. The electronic clouds of solvent molecules surrounding the solute deformate in response to the solute dipole moment. The resulting electronic polarization is very fast with respect to the relevant degrees of freedom of the solute. As a consequence, the dynamics of the electronic polarization is irrelevant to our discussion⁹. The second contribution to the reaction field originates from the reorientation of the (polar) solvent molecules around the solute. This contribution, that of course vanishes in non-polar solvents, is slower than the solute degrees of freedom^{6,7}. It is responsible for the large solvatochromic behavior of push-pull

chromophores⁵ and dominates the temporal evolution of observed spectra in time-resolved experiments¹.

In a typical time-resolved experiment the system is shot by a pulse, or a series of pulses, that induces a transition between the ground and the excited state (or viceversa). During this process the solvent molecules have not time to reorient in response to the sudden change of the solute dipole moment, and an out of equilibrium (orientational) polarization is generated. Provided the state generated by impulsive excitation lives long enough, the orientational contribution to the reaction field (F_{or}) slowly evolves from its initial value (i.e. that equilibrated with the solute dipole moment before excitation), towards the equilibrium value for the state reached upon excitation. Within linear perturbation theory, the energy of the states involved in the transition is linearly affected by the reaction field, and the frequency of the relevant transition acquires a linear dependence on the reaction field: $\hbar\omega(F_{or}) = \hbar\omega(F_{or} = 0) - F_{or}(\mu_E - \mu_G)$, where $\mu_{G(E)}$ is the electric dipole moment of the ground (excited) state⁶. Then, the experimentally accessible temporal evolution of the transition frequency, $\omega(t)$, gives direct information on the temporal evolution of the orientational solvent polarization.

The continuum dielectric model reduces the highly irregular and complex motion of the solvent molecules to the motion of a single effective solvation coordinate, the reaction field¹⁰. The dynamical behavior of this special coordinate is subject to large frictional random forces, that guarantee for an energy dissipation mechanism⁴. In the hypothesis of large friction (overdamped motion) the resulting dynamics is very simple. The solvation correlation function (also called the spectral correlation function),

$$C(t) = \frac{\omega(t) - \omega(\infty)}{\omega(0) - \omega(\infty)} \quad (1)$$

has in this hypothesis a simple exponential form, and the corresponding relaxation time, τ_S , coincides with the longitudinal relaxation time, τ_L , of the pure solvent¹. Deviations from this simple behavior are expected in the case of low-friction or when the translational motion of solvent molecules dominates over orientational motion^{1,11}.

Extensive experimental work has been devoted by several groups to collect time-resolved spectra of polar chromophores in solution^{12,13,14,15,16,17,18,19,20,21,22,23}. The interpretation of experimental data proved more difficult than described in the simple picture summarized above. First of all a finite contribution to the Stokes shift ($\omega(0) - \omega(\infty)$) is given by the vibrational degrees of freedom of the solute molecule, as demonstrated most clearly by the observation of finite Stokes shifts for chromophores dissolved in non-polar solvents. Internal vibrational coordinates are in fact slower than electronic degrees of freedom, and hence contribute to the Stokes shift. However, thanks to the different timescales of vibrational and solvation motions, their contributions to the temporal evolution of spectra can be at least approximately separated¹⁶. The basic idea is that, after impulsive excitation, vibrational degrees of freedom relax almost instantaneously with respect to solvation timescales, so that vibrational relaxation is essentially done before solvent relaxation starts. Accordingly, the zero-time frequency, $\omega(0)$, to be inserted into Eq. (1), is not the true zero-time frequency, i.e. that relevant to the unrelaxed (vertical) system, but represents the frequency measured at an effective zero-time for the solvation motion, i.e. the hypothetical time when vibrational coordinates are fully relaxed, but the solvent is still frozen in its vertical configuration. This effective $t = 0$ time, first introduced by Maroncelli and coworkers in the analysis of time-resolved fluorescence spectra²⁴, has no experimental counterpart, and $\omega(0)$ cannot be measured directly. Maroncelli proposed a clever approach to extract $\omega(0)$ from experimental steady-state spectra collected in polar and apolar solvents²⁴. The procedure unavoidably introduces uncertainties in the estimated $\omega(0)$ that add to the uncertainties in the frequencies estimated from the broad and asymmetric fluorescence bands¹³. Precise estimates of $C(t)$ are therefore difficult. On a more fundamental vein, the simplest solvation model outlined above, and, *a fortiori*, the approach suggested by Maroncelli, both rely on the hypothesis of instantaneous vibrational relaxation and on the hypothesis of an ideal solvation probe: i.e. of a molecule whose spectral properties are largely affected by the surrounding medium, but whose presence does not affect the solvent dynamics. The assumption of a complete separation of vibrational and solvation time-scales is expected to work well unless one is interested in the very early times of solvation (the first few tens of femtoseconds). Deviations can be predicted for molecules with very slow (conformational) degrees of freedom, particularly if solvents with very fast relaxation dynamics are considered. The assumption of the solvent response being unaffected by the perturbing solute is only valid in the linear regime for the solute-solvent perturbation. But linear approaches are inadequate to treat solvation of push-pull chromophores. Just in view of the strong absorption in the visible region, in fact, push-pull chromophores have large polarizabilities (and hyperpolarizabilities): the reaction field then not only affects the

solute energy, but also its dipole moment. The dipole moment in turn affects the reaction field in a feedback mechanism that is responsible for large non-linearity.

In recent years we have developed a simple yet powerful method to describe steady-state electronic and vibrational spectra of polar chromophores in solution^{25,26,27,28}. The solute is described in terms of two electronic states linearly coupled to internal vibrations (Holstein coupling) and to the reaction field⁹. This model allows for non-perturbative solutions and naturally describes several features of experimental spectra that were not understood in standard linear approaches. The reliability of the model is proved by extensive comparison with steady-state electronic and vibrational spectra collected for several chromophores in different solvents^{28,29,30}. In this paper we extend the model to describe time-resolved spectra. In particular we show that accurate time-resolved spectra of polar-polarizable chromophores can be calculated adopting the same set of parameters used for steady-state spectra without the need to introduce additional adjustable parameters. Working in the hypothesis of a complete separation of solvation and vibrational dynamics, the model accounts for deviations of $C(t)$ from the simple exponential form, and rationalizes the observation of time-dependent band-shapes and the appearance of temporary isosbestic points (TIPs). These characteristic features of time-resolved spectra of polar-polarizable chromophores^{19,20,21,22,23}, are a direct consequence of the solute (hyper)polarizability, and cannot be rationalized within the standard linear picture for solvation outlined above. As a matter of fact these features have often been taken as evidences of the failure of the continuum solvation model^{13,14,15} or for the failure of the two-state description of the chromophore²³. We demonstrate instead that they can appear as natural consequences of the molecular polarizability and can be described within the simplest model for solvation, provided the fundamental interactions of electronic degrees of freedom with molecular vibrations and with the solvent reaction field are treated beyond linear perturbative approaches.

II. THE MODEL

We consider two electronic states linearly coupled to molecular vibrations and to solvent degrees of freedom, according to the following Hamiltonian⁹:

$$\mathcal{H} = 2z_0\hat{\rho} - t \sum_{\sigma} \left(a_{D,\sigma}^{\dagger} a_{A,\sigma} + a_{A,\sigma}^{\dagger} a_{D,\sigma} \right) + \sum_i \left[\frac{1}{2} (P_i^2 + \omega_i^2 Q_i^2) - \sqrt{2\epsilon_i} \omega_i Q_i \hat{\rho} \right] \quad (2)$$

where the first two terms describe the electronic problem, with $\hat{\rho} = \sum_{\sigma} a_{A,\sigma}^{\dagger} a_{A,\sigma}$ counting electrons on A site, and $a_{A,\sigma}^{\dagger}$, $a_{D,\sigma}^{\dagger}$ creating an electron with spin σ on D and A site, respectively. Q_i and P_i , with $i > 0$, are

the coordinates and conjugated momenta describing the coupled vibrations of the chromophore, and Q_0 is the effective solvation coordinate. All coordinates are harmonic, with frequency ω_i ; the relevant relaxation energy is ϵ_i . In the following we explicitly account for a single coupled vibration, Q_1 . This simplifies equations and limits the number of adjustable parameters in the model, with no major loss of accuracy in the calculation of electronic spectra²⁸. The extension to the multimode case is possible, and interesting effects of the mixing among different vibrational coordinates are indeed expected in vibrational spectra^{27,30}.

In the adiabatic approximation, the Hamiltonian in Eq. (2) can be diagonalized at fixed Q_i 's on the basis of $|DA\rangle$ and $|D^+A^-\rangle$ states^{9,31}. The resulting ground and excited states are fully defined in terms of a single Q_i -dependent parameter, $\rho = \langle G|\hat{\rho}|G\rangle$, as follows:

$$\begin{aligned} |G\rangle &= \sqrt{1-\rho}|DA\rangle + \sqrt{\rho}|D^+A^-\rangle \\ |E\rangle &= -\sqrt{\rho}|DA\rangle + \sqrt{1-\rho}|D^+A^-\rangle \end{aligned} \quad (3)$$

The corresponding energies define the multidimensional ground and excited state potential energy surfaces (PES), as shown in Fig. 1a. The calculated PES are interesting in several respects. All coordinates inserted into the Hamiltonian are harmonic, and no term appears into Eq. (2) explicitly accounting for the mixing of different coordinates. The PES in Fig. 1 are instead clearly anharmonic and indicate a large mixing between the two involved coordinates. The softening of the ground state PES, and the hardening of the excited state PES are also recognized. All these effects are due to the coupling of the Q_i 's to the electronic system²⁷. In particular we underline that the coupling between vibrational and solvation coordinates stems out naturally from their common coupling to the electronic system.

The PES in Fig. 1 represent the potential for the motion of slow coordinates, Q_i 's. Internal vibrations with typical frequencies in the mid-infrared region, are true quantum-mechanical objects. The relevant anharmonic problem defined by the PES in Fig. 1 has been solved numerically, and large effects of the anharmonicity of internal vibrational modes have been demonstrated in static hyperpolarizabilities^{32,33}. On the contrary, vertical processes, like, e.g., absorption and emission are hardly affected by anharmonicity^{32,34,35}. In particular, vertical processes are quite accurately described by replacing the two anharmonic PES by the two parabolas that best fit the ground and excited state PES in the relevant region of the Q space (best harmonic approximation^{32,33,34}). Of course the role of anharmonicity can be recognized in the variation of the effective harmonic parameters fitting absorption and emission processes in this local-harmonic approximation.

Within the local harmonic approximation, electronic spectra and their variation in the Q -space are fully defined in terms of ρ . The vertical transition frequency and

the transition dipole moment are^{25,27}:

$$\begin{aligned} \hbar\omega_{CT} &= \frac{\sqrt{2}t}{\sqrt{\rho(1-\rho)}} \\ \mu_{CT} &= \mu_0\sqrt{\rho(1-\rho)} \end{aligned} \quad (4)$$

where μ_0 is the dipole moment of $|D^+A^-\rangle$. The Huang-Rhys (HR) factor for the coupled vibrational coordinate (Q_1) is^{25,27}:

$$\lambda_1 = \frac{\epsilon_1}{\hbar\omega_1}(1-2\rho)^2 \quad (5)$$

Based on Eqs. (4) and (5), absorption and emission spectra at any specified position in the Q space are calculated as²⁸:

$$\mathcal{S}(\omega) \propto \omega^M |\mu_{CT}|^2 \sum_n \frac{\lambda_1^2}{\sqrt{n!}} I(\omega - \omega_n) \quad (6)$$

where ω_n is the frequency of the n -th vibronic line, and $I(\omega)$ is the intrinsic line-shape function that we choose as a Gaussian with standard deviation σ . $M = 1, 3$ for absorption and emission, respectively.

The solvation coordinate describes the slow orientational motion of polar solvent molecules around the polar solute. The relevant coordinate, Q_0 , can then be treated as a classical coordinate, and, at finite temperature, it is responsible for inhomogeneous broadening. Since the solvation motion is coupled to electronic degrees of freedom, and, through them, to internal vibrations, inhomogeneous broadening has in these systems quite peculiar features. Due to thermal disorder in fact, the solution can be thought of as a collection of chromophores each one surrounded by a slightly different Q_0 configuration. Both electronic and vibrational motions are very fast if compared to solvation, so that each solute molecule readjusts instantaneously its polarity and its geometry in response to the local Q_0 configuration²⁷. Thermal disorder in Q_0 is then responsible for disorder in electronic and vibrational properties, that shows up in electronic and vibrational spectra, and, most apparently, in the anomalous dispersion of resonant Raman frequencies with the excitation line^{27,29}. With reference to Fig. 1, the thermally equilibrated state in either the ground or excited state PES is defined in terms of a Boltzmann distribution of states lying along the dashed lines drawn across the isopotential lines in Fig. 1b and 1c to mark the local minimum path with respect to the vibrational coordinate. The steady-state absorption and emission spectra are then sums of the contributions in Eq. (6) calculated for each point along the minimum path in the ground state and excited state PES, respectively, and weighted by the relevant Boltzmann distribution^{27,28}.

This simple model has been applied successfully to describe electronic and vibrational spectra of several chromophores, reproducing many features of experimental spectra that were not understood before^{28,29,30}. Just as an example, Fig. 2A and 2B shows the absorption and

emission spectra calculated in the proposed approach to fit experimental spectra of DCM dissolved in several solvents. These spectra accurately reproduce experimental data²⁸, and deserve some comment. The red-shift of absorption and emission bands with increasing solvent polarity (positive or normal solvatochromism) is typical of chromophores with a neutral ground state ($\rho < 0.5$)⁵. For these chromophores the solute polarity increases upon excitation, and the excited state is stabilized by a polar surrounding medium. The evolution of the bandshape with the solvent polarity is a more subtle phenomenon that can be understood only if the polarizability of the solute is accounted for^{27,28}. In fact, the polarity of the (polarizable) solute increases with the polarity of the surrounding medium. For neutral chromophores then ρ increases towards 0.5, and HR factors decrease: even if inhomogeneous broadening increases with the solvent polarity, absorption and emission bands apparently narrow, since the underlying vibronic profile narrows (λ_1 decreases, see Eq. (5)). For zwitterionic chromophores ($\rho > 0.5$), instead, the ionicity increases towards 1, and HR factors increase with the solvent polarity: in this case the effects of solvent polarity on inhomogeneous broadening and HR factors sum up to widen absorption and emission bands. This behavior is experimentally verified in dyes with inverse solvatochromism^{20,37,38}, and is reproduced in Fig. 2C and 2D for a hypothetical dye with the same molecular parameters as DCM, but a different z_0 , as to have a zwitterionic ground state.

Another direct consequence of the molecular polarizability is recognized in the non-specularity of steady-state absorption and emission bands^{25,28}. The behavior is similar for neutral and zwitterionic chromophores, with narrower emission than absorption bands. In all chromophores, in fact, the mixing between the two basis states increases in the relaxed excited state, so that, in both cases steady-state emission spectra correspond to states with ρ nearer to 0.5 than states relevant to absorption spectra. According to Eq. (5), HR factors for emission are always smaller than for absorption then justifying quite naturally the observed narrowing of emission bands.

III. RELAXATION DYNAMICS

The success of the two-state model in reproducing steady-state absorption and emission spectra invites modeling time-resolved experiments, as related to the dynamics of non-equilibrium states created by impulsive excitation in either the ground or excited state PES. We are not interested in the fast relaxation of vibrational coordinates (typically accomplished within few tens of femtoseconds after excitation)^{16,22}, rather we model the slower solvation dynamics in the hundreds of femtoseconds to picosecond temporal window. The problem is therefore greatly simplified if we work in the hypothesis of a complete separation of vibrational and solvation dy-

namics. First of all, just after a (sequence of) pulse(s) has created an out of equilibrium state in one of the PES, an instantaneous relaxation of vibrational coordinates takes place before solvation relaxation starts¹⁶. Moreover, during the subsequent relaxation of solvation degrees of freedom, internal coordinates immediately readjust with respect to the instantaneous configuration of the solvent. Due to the non-linearity of the coupled problem, the electronic wavefunction readjusts following Q_0 and, as a consequence, the equilibrium geometry of the chromophore varies with Q_0 . Since electronic and vibrational degrees of freedom are much faster than solvation, they are always in equilibrium with the instantaneous configuration of the solvent, and the relaxation of the effective solvation coordinate does not proceed along a horizontal line (fixed Q_1) in Fig. 1b or 1c, but follows the dashed lines drawn across the isopotential lines to mark the minimum energy path in each surface.

In a time-resolved fluorescence experiment, an impulsive excitation drives the system from the thermally equilibrated ground state (centered on point G in Fig. 1b) to the vertical excited state (point G' in Fig. 1c). After excitation, the instantaneous relaxation of vibrational degrees of freedom drives the system to point F, i.e. to the local minimum in the excited state PES, at the Q_0 relevant to the equilibrium ground state configuration. During the $G \rightarrow G' \rightarrow F$ path, the Q_0 configuration is unaffected. Once the system has reached point F, solvent relaxation starts. Since vibrational degrees of freedom follow adiabatically the solvent relaxation, the relaxation path towards the minimum of the excited state PES ($F \rightarrow E$) follows the minimum energy path, i.e. the dashed line drawn across points F and E in Fig. 1c. So, in spite of being driven by orientational degrees of freedom of the solvent, the dynamics of the system occurs along an effective coordinate that describes a concerted motion of solvation degrees of freedom and internal vibrations. Once again, the coupling between the two kinds of motion originates from their common coupling to the electronic system, and is a direct consequence of the molecular polarizability.

Time-resolved fluorescence spectra can be calculated following the same procedure described in the previous section for steady-state spectra, provided the temporal evolution of the Q_0 probability distribution is known. To such an aim we rely on a Fokker-Planck description of the dynamics of the joint probability distribution in the space of the solvation coordinate and momentum^{39,40}, $W(Q_0, P_0)$, as described by the following equation of motion:

$$\frac{\partial W}{\partial t} = -\dot{Q}_0 \frac{\partial W}{\partial Q_0} - \dot{P}_0 \frac{\partial W}{\partial P_0} + \gamma \left\{ W + P_0 \frac{\partial W}{\partial P_0} + kT \frac{\partial^2 W}{\partial P_0^2} \right\} \quad (7)$$

where γ is the phenomenological friction coefficient for the motion along the relevant relaxation path. Starting from point F, where the distribution is rigidly translated from the equilibrium ground state distribution, the Fokker-Planck equation can be easily integrated along

the F-E path in Fig. 1c. The calculation can be simplified by recognizing the overdamped nature of the solvation coordinate ($\gamma \gg \omega_0$). In the overdamped regime, the momentum rapidly attains the equilibrium, so that it needs not to be considered as an independent dynamic variable⁴⁰. The only relevant dynamics involves the Q_0 -distribution, $w(Q_0)$, as described by Smoluchowski equation:

$$\frac{\partial w}{\partial t} = \frac{1}{\gamma} \left[w \frac{\partial^2 V}{\partial Q_0^2} + \frac{\partial V}{\partial Q_0} \frac{\partial w}{\partial Q_0} + kT \frac{\partial^2 w}{\partial Q_0^2} \right] \quad (8)$$

where $V(Q_0)$ is the (classical) potential for the Q_0 motion. We verified that for $\gamma > 2\omega_0$ the Smoluchowski equation leads to the same results as the Fokker-Planck equation. Apart from a simplification in the integration procedure, working in the overdamped limit has the advantage of reducing the number of free parameters required to model solvation dynamics. In fact, as it is well known⁴⁰ and as we have explicitly verified, in that limit all dynamic properties depend on γ and ω_0 only through the ratio $\tau = \gamma/\omega_0^2$. τ represents an effective solvation time, and can be fixed as the longitudinal relaxation time (τ_L) of the pure solvent¹.

Fig. 3 shows time-resolved spectra calculated for DCM dissolved in two different solvents (CH_3CN and CHCl_3). All molecular parameters, and the solvent relaxation energies as well, are kept fixed at the values previously obtained from the fit of steady-state spectra²⁸ (cf Fig. 2, left panels). According to literature data, we fix $\tau = 0.3$ and 2.8 ps for CH_3CN and CHCl_3 , respectively¹⁶. The spectra in Fig. 3 compare nicely with experimental spectra^{17,18}, and accurately reproduce the progressive red-shift of the band, as well as its narrowing. In order to better understand the origin of the evolution of band-shapes during solvation, Fig. 4 shows time-resolved spectra calculated for the same parameters as Fig. 3A, but without accounting for inhomogeneous broadening, i.e. by collapsing the $w(Q_0)$ distribution into a δ -function. The comparison between inhomogeneously broadened spectra in Fig. 3A and homogeneous spectra in Fig. 4 demonstrates that the evolution of the band-shape accompanying the solvent relaxation is essentially due to the evolution of the vibronic structure (i.e. of HR factors), and reflects quite naturally the evolution of the molecular geometry along the relaxation path. The $w(Q_0)$ distribution, obtained from the solution of the Smoluchowski equation, also evolves with time, but it affects calculated spectra in a more subtle way. In fact $w(Q_0)$ is responsible for inhomogeneous spectral broadening, whose temporal evolution is hardly recognized in the fairly broad emission spectra of polar chromophores in polar solvents.

Similar features, including the progressive red-shift of the emission band and its narrowing, are recognized in time-resolved emission spectra of many other dyes, including neutral dyes like coumarin 153¹⁶, and zwitterionic dyes like LDS-750¹². In fact, in spite of the opposite solvatochromism, neutral and zwitterionic dyes are

predicted to have similar behavior with respect to time-resolved emission, as demonstrated by the time-resolved spectra calculated in Fig. 5 for the same zwitterionic dye whose steady-state absorption and emission spectra are reported in Fig. 2, right panels. Both the red-shift and the narrowing of time-resolved emission bands are due to the increase of the mixing between the two basis states during the relaxation of the system along the effective solvation coordinate, as discussed in the previous section with reference to steady-state spectra.

Other time-resolved experiments can be described within the proposed approach. Transient hole-burning experiments have been designed to follow the relaxation along the ground state PES. Specifically, we make reference to the experiment described in Ref. 22. In this experiment, a solution of coumarin 102 (C102) dissolved in CH_3CN is impulsively excited to transfer population from the minimum of the ground state PES (point G in Fig. 1b) to the vertical excited state (point G' in Fig. 1c). After a delay time long enough as to allow for the complete relaxation of the system in the excited PES (from G' to E in Fig. 1c), a second dump pulse is applied to vertically transfer the equilibrated population in the excited state PES into the ground state PES (from E to E' in Fig. 1b). We are not interested in modeling the initial relaxation of vibrational coordinates occurring during the first few tens of fs²², but, much as it was done for time-resolved fluorescence, we want to model the slower spectral evolution due to the solvent relaxation. We then assume an instantaneous (within the relevant solvation timescale) relaxation along the vibrational coordinate, towards point R in the ground state PES (Fig. 1b) lying on the local minimum path with respect to Q_1 . The calculation of transient absorption spectra then goes via the solution of the Smoluchowski equation for $w(Q_0)$ from time zero (where the equilibrium $w(Q_0)$ relevant to the excited state PES is rigidly translated to point R in the ground state PES) towards the ground state equilibrium in G.

Figure 6 shows transient differential absorption spectra calculated for C102 in CH_3CN . Molecular parameters for C102, as well as the solvent relaxation energy relevant to C102 in CH_3CN , are obtained from the fit of steady-state absorption and emission spectra⁴¹. The additional parameter entering the Smoluchowski equation, τ , is again fixed to 0.3 ps. In order to compare directly with experimental results, the upper and lower panel in Fig. 6 report the spectra calculated in two different temporal windows. The comparison with experimental spectra in Fig. 5 of Ref. 22 is very good: in particular we reproduce not only the blue-shift of the band, but also the appearance of a TIP, and its temporal evolution. The origin of TIPs is easily recognized in the variation of the band-shape of the transient absorption that accompanies its progressive blue-shift. Whereas the rigid translation to the blue of the transient absorption band is quite easily understood based on the simplest linear model for solvation, the temporal evolution of the band-shape is

a direct consequence of the molecular polarizability. In fact, as long as the system relaxes along the R-G path in Fig. 1b, the molecule readjusts its polarity (from $\rho \sim 0.23$ to 0.16, in the specific case of C102 in CH_3CN), and HR factors relevant to the absorption process change with time. TIPs are puzzling features of time-resolved spectra that cannot be explained easily within the standard picture for solvation, but are a natural consequence of the polarizability of the solute molecule.

TIPs appear quite commonly in pump-probe experiments^{19,20,21,23}. In these experiments, after the application of a pump pulse that drives the system to the excited state PES, the variation of the optical density of the solution is monitored by a probe-beam as a function of the delay time after the pulse. The experiment is easier than the hole-burning experiment, but the interpretation of resulting spectra is more complex. In fact at least three processes can contribute to the observed signal at each frequency. Both the bleaching of the absorption from the ground state (due to the reduced ground state population) and stimulated emission decrease the optical density, leading to a negative signal, whereas the absorption from the excited state increase the optical density, originating a positive signal. A reasonable separation of the different contributions is only possible if the three processes occur in well separated spectral regions. For polar chromophores in polar solvents, the large Stokes-shifts guarantee in general a reasonable discrimination between signals originating from the bleaching of the ground state absorption and from stimulated emission. If the positive signal from excited state absorption does not interfere too much, the pump-probe experiment gives information on the evolution of the emission band during the relaxation of the system along the F-E path in the excited state PES (Fig. 1c), so that, in favorable cases, the pump-probe experiment gives similar information as time-resolved fluorescence. According to the previous discussion, we then predict a progressive red-shift and narrowing of the emission band, in quite good agreement with available experimental data for several chromophores, with either a neutral^{19,21,23} or a zwitterionic ground state²⁰. We underline once more that the red-shift of the stimulated emission band is easily rationalized in the standard solvation model. On the opposite, the narrowing of the band, being related to the variation of the molecular polarity with the solvent relaxation, can only be understood in models where the molecular polarizability is properly accounted for. The concomitant red-shift and narrowing of the emission band are responsible for the appearance of TIPs in observed spectra.

IV. DISCUSSION

Push-pull chromophores are interesting molecules in several respects: they find application as solvation probes^{2,5}, as laser-dyes, and as chromophores for

non-linear optics⁴². They are also good two-photon absorbers⁴³ and work as molecular rectifiers⁴⁴. From a theoretical point of view, the possibility to describe the electronic structure of these molecules in terms of an effective two-state model makes these systems fascinating model systems to understand electron-transfer in solution and specifically to investigate the physics of solvation in electron-transfer processes^{4,45,46,47}. In a series of recent papers^{9,25,27,28}, we have extended the standard two-state model for push-pull chromophores^{48,49,50} to account for solvation and molecular vibration. The model allows for a non-perturbative treatment of the relevant couplings and fully accounts for the solute (hyper)polarizability, yielding to a successful picture for steady-state spectra of push-pull chromophores in solution^{28,29,30}. Here we extend the model to time-resolved spectra and demonstrate the important role of the solute hyperpolarizability in several characteristic and non-trivial spectroscopic features.

Consider a simple system with no electron-vibration coupling. Due to the molecular (hyper)polarizability, the reaction field affects the solute properties and, in turn, is affected by the presence of the solute. As a consequence of this feedback interaction, the ground and excited state PES for the Q_0 motion are deformed³⁵. The linear polarizability ($\alpha_{G/E}$) is responsible for a renormalization of the relevant harmonic frequencies²⁷:

$$\Omega_{G/E} = \omega_0 \sqrt{1 - 2\epsilon_0 \alpha_{G/E} / \mu_0^2} \quad (9)$$

while higher order polarizabilities originate anharmonic corrections^{32,33} that can be fairly large for chromophores with large NLO responses. The role of the molecular first polarizability, α , on solvation dynamics is easily understood and has already been discussed by several authors^{51,52,53,54}. If the hyperpolarizability is neglected, the PES are harmonic and the solvation relaxation function, $C(t)$, has a simple exponential form. The relaxation time, $\tau_{G/E} = \gamma / \Omega_{G/E}^2$, is however renormalized with respect to the relaxation time of the pure solvent, $\tau = \gamma / \omega_0^2$, and depends on specific properties of the solute. A qualitatively different behavior is expected if hyperpolarizabilities are accounted for, leading to anharmonic PES. In this case, a non-exponential $C(t)$ is expected, whose detailed behavior depends the details of the relevant PES. The role of the solute hyperpolarizabilities on solvation dynamics has not been recognized so far and the observed deviations of $C(t)$ from the simple exponential behavior have always been ascribed to the failure of the continuum model for the solvent or to the underdamped nature of the solvation coordinate^{13,14,15}. Instead a non-exponential behavior can show up within the simplest model for solvation, as a consequence of the solute hyperpolarizability.

The molecular (hyper)polarizability has even more important effects in the presence of coupled internal vibrations. In fact the common coupling of vibrational and solvation degrees of freedom to the electronic system in-

duces a mixing between the two kinds of coordinates, even if no direct coupling between the modes is included in the hamiltonian. The physical origin of the mixing lies in the molecular (hyper)polarizability: the polarizable molecule in fact readjusts its polarity to any variation of solvation or of vibrational coordinates, but this variation of polarity affects in turn all coordinates, leading to an interdependence of all motions. As discussed in the previous section, even in the simplifying hypothesis of a complete separation of the timescales of vibrational and solvation motion, the relaxation of the solvent coordinate always implies, for a polarizable solute, a concomitant relaxation along the vibrational coordinates. Therefore time-resolved experiments performed on polarizable chromophores measure a complex motion where the molecular geometry readjusts following the solvent relaxation. Deviations of the observed relaxation time from the relaxation time of the pure solvent, as well as deviations from the simple exponential behavior for $C(t)$, are obviously predicted in this model. Just as an example, Fig. 7A compares the spectral correlation function calculated for hole-burning experiment on C102 described in the previous section. Deviations of the exact result from the simple exponential behavior, as well as an overall slowing down of the solvation dynamics with respect to the pure solvent, can be appreciated from the figure, even if, due to the large experimental uncertainties in $C(t)$, they are possibly too small to be safely identified in experimental data. Larger effects are predicted for more polarizable solute molecules, as shown in Figure 7B for phenol blue, an interesting solvatochromic probe whose large hyperpolarizability is known since date⁵⁵. Quite irrespective of their magnitude, these effects are important since they demonstrate that the presence of a polarizable solute affects solvation dynamics: the relaxation time obtained from the spectral relaxation function is not a property of the pure solvent, but also depends on the solute molecule. Good solvation probes should be largely solvatochromic and *hardly polarizable* as well.

The two-state model unavoidably assigns the excited state a linear polarizability equal in magnitude and opposite in sign to the ground state polarizability, then pointing to a solvation time in the excited state smaller than the longitudinal relaxation time of the pure solvent. As discussed in Ref. 56 the negative polarizability of the excited state is probably an artifact of the two-state model, that neglects the mixing of the low-lying excited state with higher excited states whose (positive) contribution to α_E usually over-compensate the negative contribution from the mixing with the ground state. Estimates of excited state polarizabilities are available for just a few chromophores and all confirm positive α_E values^{57,58}. However, the possibility of observing a negative α for the excited state of highly polarizable chromophores cannot be excluded a priori. In any case, it is possible to modify the proposed approach to account for the role of (a few) higher excited states. However, this would introduce new adjustable parameters in the model, whose definition is

arbitrary in the absence of accurate experimental information on the polarizability of the excited state, or on the relaxation dynamics in the excited state.

The analysis of $C(t)$ is hindered by large experimental uncertainties, and the effects of the solute (hyper)polarizability are more easily recognized in the temporal evolution of band-shapes. As recently suggested by Matyushov⁵⁴, if one accounts for the solute linear polarizability, the different curvatures in the ground and excited state PES lead to different equilibrium $w(Q_0)$ distributions in the two states. Then a temporal evolution of $w(Q_0)$ is easily predicted in time-resolved experiments, resulting in an evolution of the inhomogeneous broadening profiles in observed spectra. The solute hyperpolarizability makes the phenomenon more complex: anharmonic PES, as originated by non-linear polarizabilities^{32,33}, in fact lead to non-Gaussian distribution profiles. However, it is important to recognize that, as discussed in the previous section, band-shapes are actually governed by vibronic profiles, inhomogeneous broadening being only responsible for their smearing out. The observed evolution of band-shapes is indeed originated by the coupling between solvation and vibrational degrees of freedom, as induced by the molecular (hyper)polarizability. The role of vibronic profiles in defining observed band-shapes was recognized in Ref. 59, but the temporal evolution of HR factors was introduced *ad hoc*. We demonstrate instead that it is a natural consequence of the solute (hyper)polarizability.

The evolution of band-shapes that accompanies the red- (blue-) shifts of time-resolved fluorescence (absorption) bands can be responsible for a crossing of observed spectra. The resulting TIPs are not true isobestic points, as their location smoothly varies with time. In any case, the appearance of TIPs has puzzled experimentalists and theorists since date^{19,20,22,23}. Recently, a paper appeared aimed to demonstrate the failure of the two-state picture for push-pull chromophores, based on the appearance of TIPs in pump-probe spectra²³. In this paper, TIPs are ascribed to a barrier-activated reaction occurring in the excited state towards a transient emissive product. Whereas further theoretical and experimental work is needed to settle this point, we underline that the molecules investigated in Ref. 23 are among the best chromophores for NLO, and are therefore largely (hyper)polarizable. The observed large deviations of relaxation times from the longitudinal relaxation times of the pure solvents, point quite nicely to deviations from the standard linear perturbative picture of the solute-solvent interaction and perfectly fit within our two-state model for polar-polarizable chromophores, and suggest an alternative explanation of TIPs.

V. CONCLUSIONS

Time-resolved spectra of polar-polarizable chromophores in solution are described based on a contin-

uum solvation model. A two-state picture is adopted for the solute, and linear coupling to internal vibrations is also accounted for. The model, originally developed to account for NLO responses^{9,31} and steady-state spectra^{25,27} of push-pull chromophores in solution, is extended here to describe time-resolved spectra. The comparison with experimental data confirms that the proposed model quite successfully grasps the essential physics of polar-polarizable chromophores in solution. The model presents some obvious drawbacks. The two-state picture must be extended to account for higher-energy states if detailed information is required on excited state properties. Moreover, the Holstein model for electron-vibration coupling only accounts for linear terms: quadratic coupling is expected to be important in cases when a very different geometry (and hence very different bond orders) can be attributed to the two basis states. Again the extension of the model in this direction is easy, but requires detailed spectroscopic information to fix all the model parameters. Finally, the continuum model for solvation has serious limitations, particularly in cases where large site-specific interactions (like, e.g., H-bonds) are expected. The hypothesis of complete separation of vibrational and solvation time-scales can fail for molecules with particularly slow internal degrees of freedom and/or for solvents with a very

fast dynamics. In spite of these limitations, and quite irrespective of its applicability to some specific systems, the proposed model opens the way to obtain exact, non-perturbative solutions of the solvation problem also in the presence of electron-vibration coupling. The spectral consequences of the molecular (hyper)polarizability, that is unavoidably neglected in the standard linear perturbative approach to solvation, are important and non-trivial, and show up quite consistently in steady-state and time-resolved spectra of push-pull chromophores. In particular here we have demonstrated that deviations from the exponential decay of the spectral relaxation function, that are usually taken as proof of the failure of the continuum model for solvation, appear quite naturally within the simplest picture, provided the molecular (hyper)polarizability is accounted for. Similarly, the temporal evolution of band-shapes, as well as the appearance of TIPS, usually ascribed to the failure of the two-state model, are another consequence of non-linearity. More complex models can of course be developed, and will lead to a better or more detailed description of spectral properties of push-pull chromophores in solution. Based on an Occam-razor approach, we believe however that the available body of experimental data does not require any more complex physics than described here.

-
- * Electronic address: terenzia@nemo.unipr.it
† Electronic address: anna.painelli@unipr.it
- ¹ J. D. Simon, *Acc. Chem. Res.* 21 (1988) 128.
 - ² G. R. Fleming, M. Cho, *Annu. Rev. Phys. Chem.* 47 (1996) 109.
 - ³ P. J. Rossky, J. D. Simon, *Nature* 370 (1994) 263.
 - ⁴ H. Heitele, *Angew. Chem. Int. Ed. Engl.* 32 (1994) 359.
 - ⁵ C. Reichardt, *Chem. Rev.* 94 (1994) 2319.
 - ⁶ W. Liptay, *Angew. Chem.* 8 (1969) 177.
 - ⁷ S. Di Bella, T. J. Marks, M. A. Ratner, *J. Am. Chem. Soc.* 4440 (1994) 116.
 - ⁸ J. N. Gehlen, D. Chandler, H. J. Kim, T. J. Hynes, *J. Phys. Chem.* 96 (1992) 1748.
 - ⁹ A. Painelli, *Chem. Phys.* 245 (1999) 183.
 - ¹⁰ R. F. Loring, Y. J. Yan, S. Mukamel, *J. Chem. Phys.* 87 (1987) 5840.
 - ¹¹ G. van der Zwan, T. J. Hynes, *J. Phys. Chem.* 89 (1985) 4181.
 - ¹² E. W. Castner Jr., M. Maroncelli, G. R. Fleming, *J. Chem. Phys.* 86 (1987) 1090.
 - ¹³ M. Maroncelli, G. R. Fleming, *J. Chem. Phys.* 86 (1987) 6221.
 - ¹⁴ S. Rosenthal, X. Xie, M. Du, G. R. Fleming, *J. Chem. Phys.* 95 (1991) 4715.
 - ¹⁵ W. Jarzeba, G. C. Walker, A. E. Johnson, P. F. Barbara, *Chem. Phys.* 152 (1991) 57.
 - ¹⁶ M. L. Horng, J. A. Gardecki, A. Papazyan, M. Maroncelli, *J. Phys. Chem.* 99 (1995) 17311.
 - ¹⁷ T. Gustavsson, G. Baldacchino, J.-C. Mialocq, S. Pommeret, *Chem. Phys. Lett.* 236 (1995) 587.
 - ¹⁸ P. van der Meulen, H. Zhang, A. Jonkman, M. Glasbeek, *J. Phys. Chem.* 100 (1996) 5367.
 - ¹⁹ S. A. Kovalenko, N. P. Ernstring, J. Ruthmann, *Chem. Phys. Lett.* 258 (1996) 445.
 - ²⁰ S. A. Kovalenko, N. P. Ernstring, J. Ruthmann, *J. Chem. Phys.* 106 (1997) 3504.
 - ²¹ S. A. Kovalenko, J. Ruthmann, N. P. Ernstring, *Chem. Phys. Lett.* 271 (1997) 40.
 - ²² S. A. Kovalenko, J. Ruthmann, N. P. Ernstring, *J. Chem. Phys.* 109 (1998) 1894.
 - ²³ P. Plaza, D. Laage, M. M. Martin, V. Alain, M. Blanchard-Desce, W. H. Thompson, T. J. Hynes, *J. Phys. Chem. A* 104 (2000) 2396.
 - ²⁴ R. S. Fee, M. Maroncelli, *Chem. Phys.* 183 (1994) 235.
 - ²⁵ A. Painelli, F. Terenziani, *Chem. Phys. Lett.* 312 (1999) 211.
 - ²⁶ A. Painelli, F. Terenziani, *Synth. Met.* 109 (2000) 229.
 - ²⁷ A. Painelli, F. Terenziani, *J. Phys. Chem. A* 104 (2000) 11041.
 - ²⁸ B. Boldrini, E. Cavalli, A. Painelli, F. Terenziani, *J. Phys. Chem. A* 106 (2002) 6286.
 - ²⁹ F. Terenziani, A. Painelli, D. Comoretto, *J. Phys. Chem. A* 104 (2000) 11049.
 - ³⁰ A. Painelli, F. Terenziani, *Synth. Met.* 116 (2001) 135.
 - ³¹ A. Painelli, *Chem. Phys. Lett.* 285 (1998) 352.
 - ³² L. Del Freato, A. Painelli, *Chem. Phys. Lett.* 338 (2001) 208.
 - ³³ L. Del Freato, F. Terenziani, A. Painelli, *J. Chem. Phys.* 116 (2002) 755.
 - ³⁴ A. Painelli, L. Del Freato, F. Terenziani, *Chem. Phys. Lett.* 346 (2001) 470.
 - ³⁵ A. Painelli, L. Del Freato, F. Terenziani, *Synth. Met.* 121 (2001) 1465.

- ³⁶ In Ref. 28 we used the same $M = 1$ exponent for both absorption and emission spectra. Since spectra are fairly broad, this slightly affects calculated emission spectra and justifies the minor differences between calculated emission spectra in Fig. 2B and those reported in Fig. 1c of Ref. 28.
- ³⁷ J. B. Baldwin, B. Chen, S. C. Street, V. V. Kononov, H. Sakurai, T. V. Hughes, C. S. Simpson, M. V. Lakshmikantham, M. P. Cava, L. D. Kispert, R. M. Metzger, *J. Phys. Chem. B* 103 (1999) 4269.
- ³⁸ X. Cao, J. L. McHale, *J. Chem. Phys.* 109 (1998) 1901.
- ³⁹ A. O. Caldeira, A. J. Leggett, *Physica* 121A (1983) 587.
- ⁴⁰ S. Mukamel, *Principles of Nonlinear Optical Spectroscopy*, Oxford University Press, New York, 1995.
- ⁴¹ A. Painelli, F. Terenziani, in preparation.
- ⁴² D. R. Kanis, M. A. Ratner, T. J. Marks, *Chem. Rev.* 94 (1994) 195.
- ⁴³ M. Albota, D. Beljonne, J.-L. Brédas, J. E. Ehrlich, J.-Y. Fu, A. A. Heikal, S. E. Hess, T. Kogej, M. D. Levin, S. R. Marder, D. McCord-Maughon, J. W. Perry, H. Röckel, M. Rumi, G. Subramaniam, W. W. Webb, X.-L. Wu, C. Xu, *Science* 281 (1998) 1653.
- ⁴⁴ R. M. Metzger, B. Chen, U. Hopfner, M. V. Lakshmikantham, D. Vuillaume, T. Kawai, X. Wu, H. Tachibana, T. V. Hughes, H. Sakurai, J. W. Baldwin, C. Hosch, M. P. Cava, L. Brehmer, G. J. Ashwell, *J. Am. Chem. Soc.* 119 (1997) 10455.
- ⁴⁵ P. F. Barbara, G. C. Walker, T. Smith, *Science* 256 (1992) 975.
- ⁴⁶ G. C. Walker, E. Åkesson, A. E. Johnson, N. E. Levinger, P. F. Barbara, *J. Phys. Chem.* 96 (1992) 3728.
- ⁴⁷ A. Myers Kelley, *J. Phys. Chem. A* 103 (1999) 6891.
- ⁴⁸ J. L. Oudar, D. S. Chemla, *J. Chem. Phys.* 66 (1977) 2664.
- ⁴⁹ D. Lu, G. Chen, G. W. Perry, W. A. Goddard III, *J. Am. Chem. Soc.* 116 (1994) 10679.
- ⁵⁰ M. Barzoukas, A. Fort, M. Blanchard-Desce, *Chem. Phys. Lett.* 257 (1996) 531.
- ⁵¹ F. Cichos, R. Brown, Ph. A. Bopp, *J. Chem. Phys.* 114 (2001) 6834.
- ⁵² B. D. Bursulaya, D. A. Zichi, H. J. Kim, *J. Phys. Chem.* 99 (1995) 10069.
- ⁵³ P. van der Meulen, A. M. Jonkman, M. Glasbeek, *J. Phys. Chem. A* 102 (1998) 1906.
- ⁵⁴ D. V. Matyushov, *J. Chem. Phys.* 115 (2001) 8933.
- ⁵⁵ S. R. Marder, D. N. Beratan, L.-T. Cheng, *Science* 252 (1991) 103.
- ⁵⁶ D. V. Matyushov, M. D. Newton, *J. Phys. Chem. A* 105 (2001) 8516.
- ⁵⁷ A. Chowdhury, D. A. Locknar, L. L. Premvardhan, L. Pelteneau, *J. Phys. Chem. A* 103 (1999) 9614.
- ⁵⁸ D. V. Matyushov, G. A. Voth, *J. Phys. Chem. A* 103 (1999) 10981.
- ⁵⁹ C.-P. Hsu, Y. Georgievskii, R. A. Marcus, *J. Phys. Chem. A* 102 (1998) 2658.
-

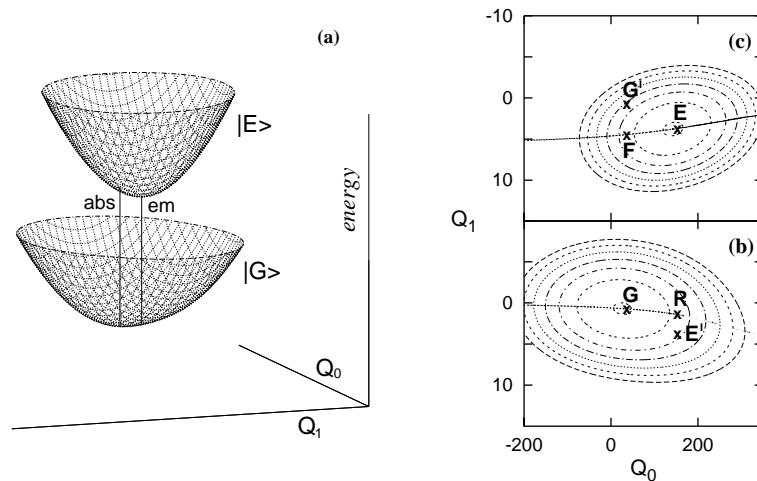


FIG. 1: (a) Potential energy surfaces calculated for the same parameters used below to fit spectra of DCM in CH_3CN : $z_0 = 1.14$ eV, $\sqrt{2}t = 0.88$ eV, $\epsilon_1 = 0.45$ eV, $\omega_1 = 0.16$ eV, $\epsilon_0 = 0.75$ eV. Q_0 and Q_1 describe the solvation and vibrational coordinate, respectively. The labels *abs* and *em* mark the vertical lines along which the absorption and emission processes occur. For the sake of clarity, the energy gap between the two surfaces has been enlarged. (b) Isopotential lines for the ground state and (c) the excited state PES shown in panel (a). Lines are relevant to equispaced energy values, the spacing corresponding to ω_1 . The dotted lines drawn across the isopotential lines mark the equilibrium Q_1 value as a function of Q_0 . Letters on the graphs mark points discussed in the text. All axes are in arbitrary units.

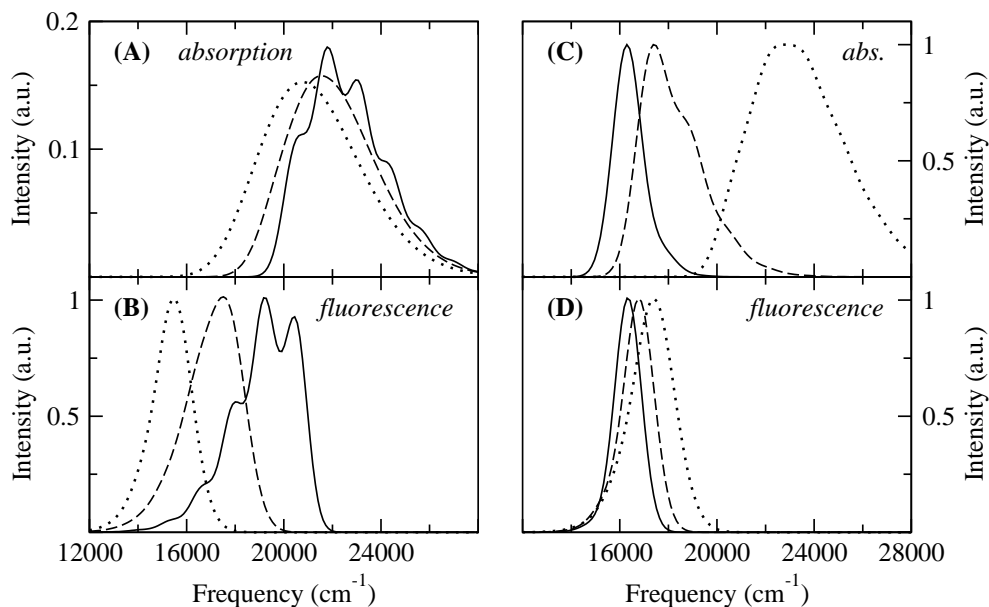


FIG. 2: Left panels: (A) Absorption and (B) fluorescence spectra calculated for DCM (same parameters of Fig. 1) in hexane (continuous lines, $\epsilon_0 = 0$), CHCl₃ (dashed lines, $\epsilon_0 = 0.32$ eV), CH₃CN (dotted lines, $\epsilon_0 = 0.85$ eV). Right panels: (C) Absorption and (D) fluorescence spectra calculated for a zwitterionic chromophore ($z_0 = 0.1$ eV, $\sqrt{2}t = 1$ eV, $\epsilon_1 = 0.5$ eV, $\omega_1 = 0.18$ eV) for $\epsilon_0 = 0$ (continuous lines), $\epsilon_0 = 0.36$ eV (dashed lines) and $\epsilon_0 = 0.85$ eV (dotted lines). The intrinsic line-width for the Gaussian associated to each vibronic feature is $\sigma = 0.06$ eV.

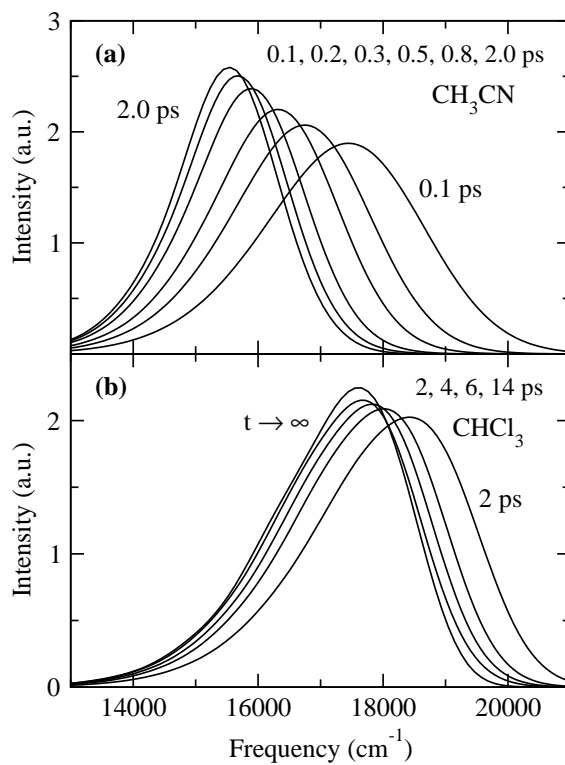


FIG. 3: Time-resolved fluorescence spectra calculated for DCM in (A) CH₃CN and (B) CHCl₃. The parameters are the same as for Fig. 2, left panels; $\tau = 0.3$ and 2.8 ps in panels A and B, respectively.

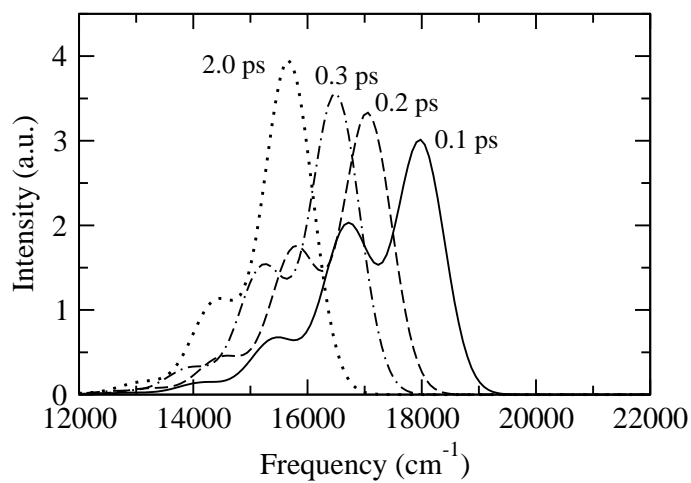


FIG. 4: The same as Fig. 3A, but without accounting for inhomogeneous broadening of the spectra. Again times relevant to the different spectra are marked on the graph.

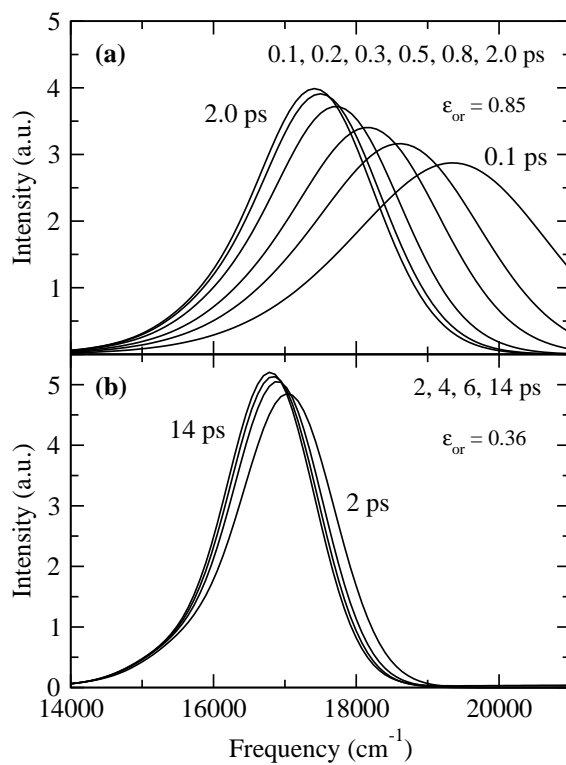


FIG. 5: The same as Fig. 3, but for the zwitterionic chromophore of right panels of Fig. 2.

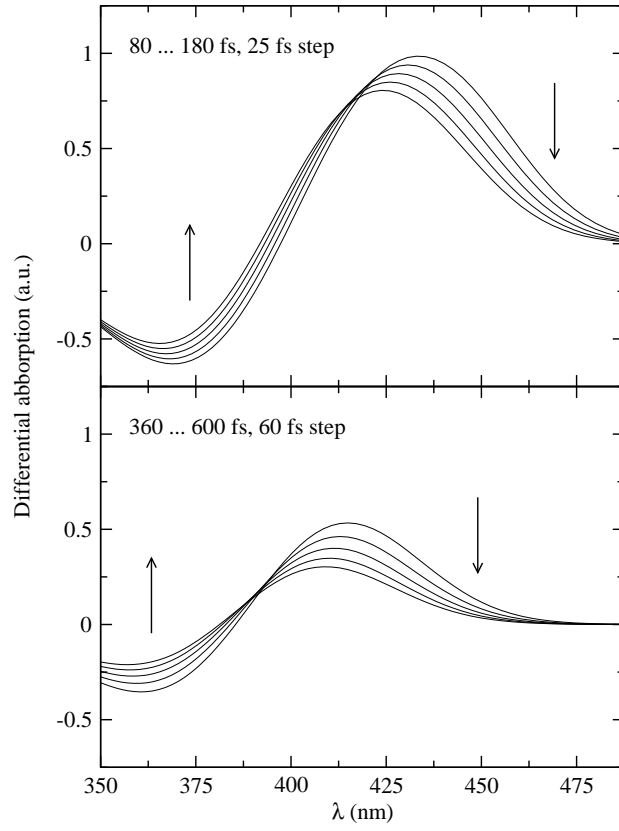


FIG. 6: Transient differential absorption spectra calculated for C102 in CH_3CN : $z_0 = 1.28$ eV, $\sqrt{2}t = 1.2$ eV, $\epsilon_1 = 0.33$ eV, $\omega_1 = 0.16$ eV, $\epsilon_0 = 0.6$ eV. Spectra are relevant to the times reported on the graphs. Calculated spectra are shown in two separate windows for a better comparison with data in Ref. 22. Arrows indicate the direction of increasing time.

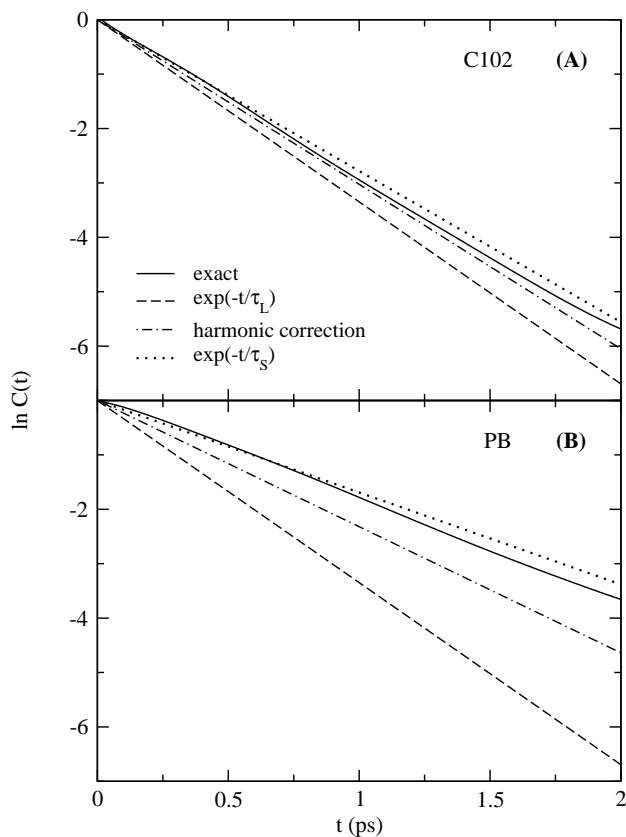


FIG. 7: Solvation correlation function for the hole-burning experiment, calculated for (A) C102 in CH_3CN (the same parameters as in Fig. 6) and (b) phenol blue in CH_3CN ($z_0 = 0.7$ eV, $\sqrt{2}t = 1$ eV, $\epsilon_1 = 0.42$ eV, $\omega_1 = 0.2$ eV, $\epsilon_0 = 0.7$ eV, from Ref. 29). Continuous lines refer to the exact results; dashed lines correspond to the non-polarizable-solute approximation; dot-dashed lines have been calculated by taking into account the linear polarizability only; dotted lines correspond to the best single-exponential fit of the exact curve.